

GRANT
IN-91-CR
38297
P-18

MODEL OF JOVIAN F REGION IONOSPHERE

(SATURNIAN IONOSPHERE MODEL IN OFFSET DIPOLE APPROXIMATION)

by

A. TAN

PRINCIPAL INVESTIGATOR

THIRD ANNUAL REPORT OF NASA GRANT NAGW-1067

(NASA-CR-188780) MODEL OF JOVIAN F REGION IONOSPHERE (SATURNIAN IONOSPHERE IN OFFSET DIPOLE APPROXIMATION) Annual Report No. 3 (Alabama Agricultural and Mechanical Coll.) 18 p

N91-31057
Unclas
CSCL 03B G3/91 0038297

RESEARCH REPORT NO. AAMU-NAG-91-3

ALABAMA AGRICULTURAL AND MECHANICAL UNIVERSITY

NORMAL, ALABAMA 35762

JULY 1991

CONTENTS

	Page
TABLE OF CONTENTS	1
1. INTRODUCTION	2
2. SATURN'S DIPOLE MODEL	3
3. THEORY	5
4. INPUT DATA	7
5. RESULTS AND DISCUSSION	8
REFERENCES	10
TABLE	11
FIGURES	12
ABSTRACT	17

1. INTRODUCTION

The influence of the earth's magnetic field on the distribution of ionization in the ionosphere is well-known. For example, the equatorial anomaly is roughly symmetrical with respect to the dipole equator rather than the geographic. Furthermore, radio occultation measurements of the Pioneer and Voyager space probes indicate the possibility of the existence of equatorial anomaly in the ionospheres of Jupiter (Mahajan, 1981) and Saturn (Mahajan, et al., 1985).

The formation of equatorial anomaly in the Jovian ionosphere under model electric fields was investigated by Tan (1986). Tan (1990) further studied the differences between the topside ionospheric profiles in the Eastern and Western Sectors of Jupiter due to the offset effect of its eccentric dipole.

In this study we investigate the offset effect of Saturn's dipole on its ionosphere. The magnetic field of Saturn is primarily that of a dipole closely aligned to the rotational axis but displaced northward from the center by a distance approximately equal to $0.05 R_S$, R_S being the reference radius of Saturn (cf. Connerney, et al., 1984). This offset effect would manifest itself most prominently between the ionospheric profiles in the Northern and Southern hemispheres of Saturn.

2. SATURN'S DIPOLE MODEL

The magnetic field of Saturn can be approximated by that of a dipole coaxial with the rotational axis and displaced from the center northward by a distance of $a = 0.05 R_S$ (Connerney, et al., 1984). The following systems of coordinates are defined in a meridional plane:

- (1) Planetocentric cartesian (x', z') ,
- (2) Planetocentric polar (r', θ') ,
- (3) Dipole cartesian (x, z) , and
- (4) Dipole polar (r, θ) coordinates.

The transformation from (r, θ) to (r', θ') is effected in the following stages: $(r, \theta) \xrightarrow{A} (x, y) \xrightarrow{B} (x', z') \xrightarrow{C} (r', \theta')$, where the transformations A, B and C are given by (vide Fig.1)

$$A: \quad x = r \sin\theta \quad , \quad (2.1)$$

$$z = r \cos\theta \quad , \quad (2.2)$$

$$B: \quad x' = x \quad , \quad (2.3)$$

$$z' = z + a \quad , \quad (2.4)$$

$$C: \quad r' = (x'^2 + z'^2)^{\frac{1}{2}} \quad . \quad (2.5)$$

$$\theta' = \tan^{-1}(x'/z') \quad , \quad (2.6)$$

Substituting Eq. (2.1) - (2.4) in (2.5) and (2.6), we get

$$r' = (r^2 + 2ar \cos\theta + a^2)^{\frac{1}{2}} \quad , \quad (2.7)$$

$$\text{and } \theta' = \tan^{-1}\left(\frac{\sin\theta}{\cos\theta + a/r}\right) \quad . \quad (2.8)$$

The inverse transformations from (r', θ') to (r, θ) are obtained by

interchanging the primed and unprimed quantities and reversing the sign of a .

$$r = (r'^2 - 2ar' \cos\theta' + a^2)^{\frac{1}{2}}, \quad (2.9)$$

$$\text{and } \theta = \tan^{-1} \left(\frac{\sin\theta'}{\cos\theta' - a/r'} \right). \quad (2.10)$$

For a dipole field line of definite L-value, the coordinates of the foot of the field line in the northern hemisphere ($r_0, \theta_0; r'_0, \theta'_0$) can be calculated given the radial distance $r'_0 = R_S + h_0 = R$ (say), where h_0 is the altitude of the base of the ionosphere. For a diffusive equilibrium model, h_0 is approximately the height of the maximum electron density. For Saturn, $h_0 = 2,500$ km (from Mahajan, 1987) and $R_S = 58,300$ km, whence $R = 60,800$ km.

The foot of the field line is the intersection of the circle $r' = R$ and the dipole field line, whose equation is

$$r = L R_S \sin^2\theta. \quad (2.11)$$

Applying Eq. (2.11) in (2.7), we get

$$L^2 R_S^2 \sin^4\theta_0 + 2aL R_S \sin^2\theta_0 \cos\theta_0 + a^2 - R^2 = 0. \quad (2.12)$$

One can solve for $y = \sin\theta_0$ numerically by the Newton-Raphson scheme (cf. Stark, 1970)

$$y'_{i+1} = y_i - \frac{f(y_i)}{f'(y_i)}, \quad (2.13)$$

$$\text{where } f(y_i) = L^2 R_S^2 y_i^4 + 2aL R_S y_i^2 (1 - y_i^2)^{\frac{1}{2}} + a^2 - R^2, \quad (2.14)$$

$$\text{and } f'(y_i) = 4L^2 R_S^2 y_i^3 + 2aL R_S \frac{y_i (2 - 3y_i^2)}{(1 - y_i^2)^{\frac{1}{2}}}. \quad (2.15)$$

3. THEORY

The topside ionospheric plasma can be approximated by a static diffusive equilibrium model $V_s = 0$, where V_s is the velocity of the ions resolved along the field line (cf. Bauer, 1969). This is even more true for the ionospheres of the major planets, where the production and loss rates are extremely slow. V_s is prescribed by the momentum equation

$$V_s = \frac{1}{m} [mg_s + mf_s - \frac{2}{N} \frac{d}{ds} (NkT)] , \quad (3.1)$$

where N = number density of electrons/ions,

m = mass of ions (H^+),

ν = ion-neutral collision frequency,

T = Temperature,

k = Boltzmann's constant,

s = arc length along dipole field line,

g_s = gravitational acceleration resolved along s ,

and f_s = centrifugal acceleration resolved along s .

Under the condition of static diffusive equilibrium, Eq. (3.1) integrates easily from the foot of the field line in the northern hemisphere to the field point

$$N = \frac{N_0 T_0}{T} e^{\int_0^s \frac{m}{2kT} (g_s + f_s) ds} . \quad (3.2)$$

The differential arc length is given by

$$ds = L R_S (3 \cos^2 \theta + 1)^{\frac{1}{2}} \sin \theta d\theta . \quad (3.3)$$

Taking into account the radial dependence of g , we have

$$g_s = - \frac{g_0 R^2}{r'^2} \sin I' , \quad (3.4)$$

where I' is the true inclination of the field line and g_0 the acceleration of gravity at the foot of the field line in the northern hemisphere.

From Fig.2, we have

$$\begin{aligned} I' &= I + \theta' - \theta \\ &= \tan^{-1}(2 \cot \theta) + \tan^{-1} \left(\frac{\sin \theta}{\cos \theta + a/r} \right) - \tan^{-1}(\tan \theta) . \end{aligned} \quad (3.5)$$

Also from Fig.2,

$$f_s = \Omega^2 r' \sin \theta' \cos(I' - \theta') . \quad (3.6)$$

Since $r' \sin \theta' = r \sin \theta$, $I' - \theta' = I - \theta$ and

$$\cos(I - \theta) = \frac{3 \cos \theta \sin \theta}{(3 \cos^2 \theta + 1)^{\frac{1}{2}}} , \quad (3.7)$$

we get, by substituting from (2.11)

$$f_s = \Omega^2 L R_S \frac{3 \sin^4 \theta \cos \theta}{(3 \cos^2 \theta + 1)^{\frac{1}{2}}} . \quad (3.8)$$

4. INPUT DATA

In the diffusive equilibrium model, it is appropriate to take the electron density at the base as the observed peak electron density. In the present study, this is assumed to be 10^4 electrons/cm³ (from Mahajan, 1987). The altitude of the base is taken as the observed height of the peak, which is roughly 2,500 km (Mahajan, 1987).

The electrons, ions and neutrals are assumed to be in thermal equilibrium (Henry and McElroy, 1969; Nagy, et al., 1976). The temperature profile is taken from the measurements of Festou and Atreya (1982), who found an isothermal region above 1450 km of constant temperature of 800 K.

The reference radius of Saturn as well as the angular velocity of rotation are taken from Mullin (1984).

5. RESULTS AND DISCUSSIONS

The diffusive equilibrium model is most appropriate for equinox conditions when both seasonal and ring effects are absent. This justifies the assumption that the base electron densities in the two hemispheres are equal.

Figures 3 through 5 illustrate the results of our calculations. In Fig.3, contour plots of the electron density in a meridional plane in the two hemispheres are shown together with the dipole field lines. In general, the electron densities are higher in the northern hemisphere than in the southern. This is a direct consequence of the dipole field line alignments in the two hemispheres. In the northern hemisphere, ionization is transported along the field lines to relatively lower altitudes than in the southern hemisphere, thus producing enhanced electron densities in the topside ionosphere.

Also shown in Fig.3 are the loci of points at which the components of gravitational and centrifugal forces along the field lines are equal and opposite. In the region of centrifugal dominance, the electron density slowly increases with distance, thus creating a region of enhanced electron density away from the planet. As a result, troughs of electron density are found at midlatitude heights ($\lambda = 25^\circ$ to 35° in the northern hemisphere and $\lambda = 25^\circ$ to 30° in the southern hemisphere) rather than above the equator. Above the equator, the electron density profile possesses a minimum which is the saddle point in the electron density contour.

Figures 4 and 5 show the vertical profiles of electron density in the two hemispheres at a midlatitude ($\lambda = 30^\circ$) and a low-latitude ($\lambda = 15^\circ$)

location. As stated earlier, the electron densities were generally greater in the northern hemisphere from the same base electron density. Consequently, the scale heights are also greater in the northern hemisphere.

The electron densities at the midlatitude locations were smaller than those at the low-latitude locations. In fact, the troughs in the electron density contour plots are located around roughly 30° latitudes in either hemisphere. At the low latitude locations, the electron density profiles undergo minima and actually increase with altitude thereafter. This would be true so long as the assumption of perfect corotation of plasma remained valid.

The calculated scale heights in the topside ionosphere for the latitudes of 15° and 30° in both hemispheres are given in Table I. The difference in the scale heights between the two hemispheres of around 200 km is significant. This difference should reveal itself if sufficient observed data become available. Also shown in the Table are the observed scale heights deduced from Voyager 2 measurements (from Mahajan, 1987) which correspond to near equinox conditions. The calculated scale heights were significantly greater than those observed, which are about 1000 km. The scale height calculated from model computations of Atreya and Waite (1981) is about 1050 km.

REFERENCES

- S. K. Atreya and J. H. Waite, Nature, 292, 682 (1981).
- S. J. Bauer, Proc. IEEE, 57, 1114 (1969).
- J. E. P. Connerney, L. Davis and D. L. Chennette in Saturn, T. Gehrels and M. S. Matthews ed., Univ. of Arizona Press (1984).
- M. C. Festou and S. K. Atreya, Geophys. Res. Lett., 9, 1147 (1982).
- R. J. W. Henry and M. B. McElroy, J. Atmos. Sci., 26, 912 (1969).
- K. K. Mahajan, Geophys. Res. Lett., 8, 66 (1981).
- K. K. Mahajan, J. Kar and M. V. Srilakshmi, Ind. J. Radio and Space Phys., 14, 143 (1985).
- K. K. Mahajan, Ind. J. Radio and Space Phys., 16, 192 (1987).
- T. S. Mullin in Saturn, T. Gehrels and M. S. Matthews ed., Univ. of Arizona Press (1984).
- A. F. Nagy, W. L. Chameides, R. H. Chan and S. K. Atreya, J. Geophys. Res., 81, 5567 (1976).
- P. A. Stark, Introduction to Numerical Methods, The MacMillan Co., New York (1970).
- A. Tan, Planet. Space Sci., 34, 117 (1986).
- A. Tan, Trans. AGU, 71, 1542 (1990).

TABLE I. CALCULATED AND OBSERVED SCALE HEIGHTS

CALCULATED SCALE HEIGHTS		
LATITUDE	HEMISPHERE	SCALE HEIGHT
15°	N	2,000 km
15°	S	1,800 km
30°	N	1,700 km
30°	S	1,500 km
OBSERVED SCALE HEIGHTS*		
LATITUDE	HEMISPHERE	SCALE HEIGHT
36°	N	1,000 km
31°	S	1,000 km

* From Mahajan (1987)

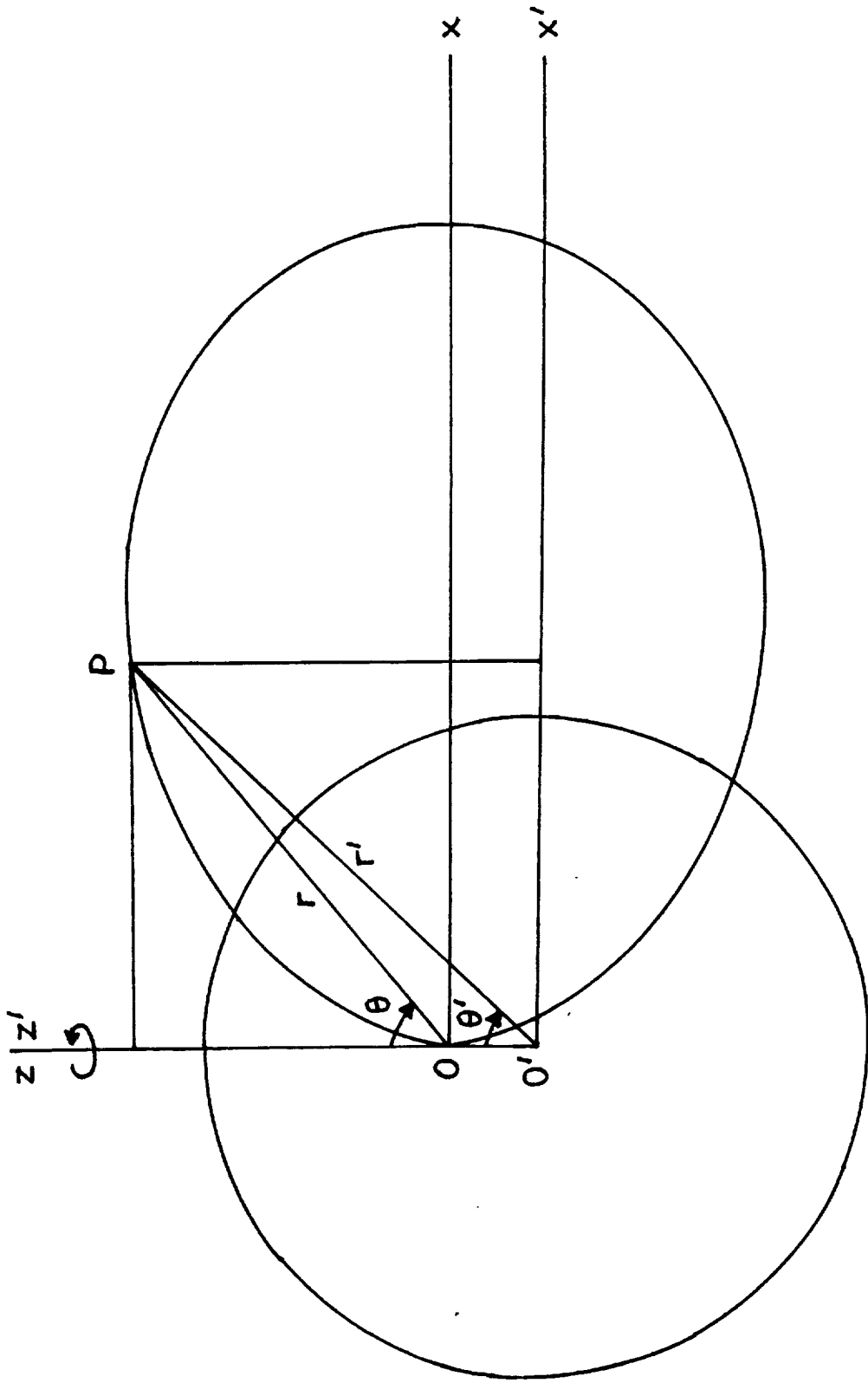


Fig.1. Planetocentric Cartesian (x', z') , Planetocentric Polar (r', θ') , Dipole Cartesian (x, z) and Dipole Polar (r, θ) Coordinates.

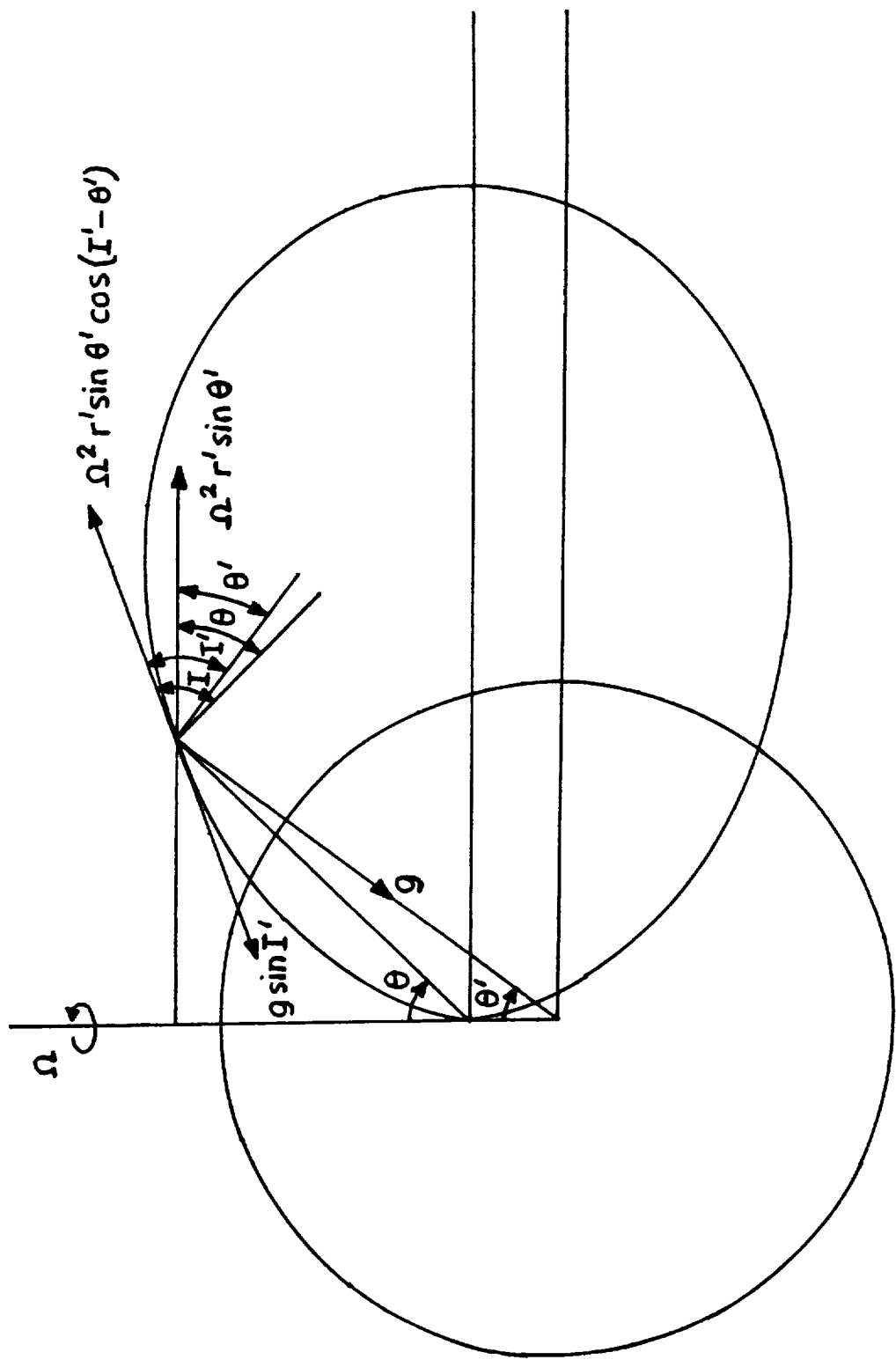


Fig.2. Components of gravitational and centrifugal accelerations resolved along the dipole field line.

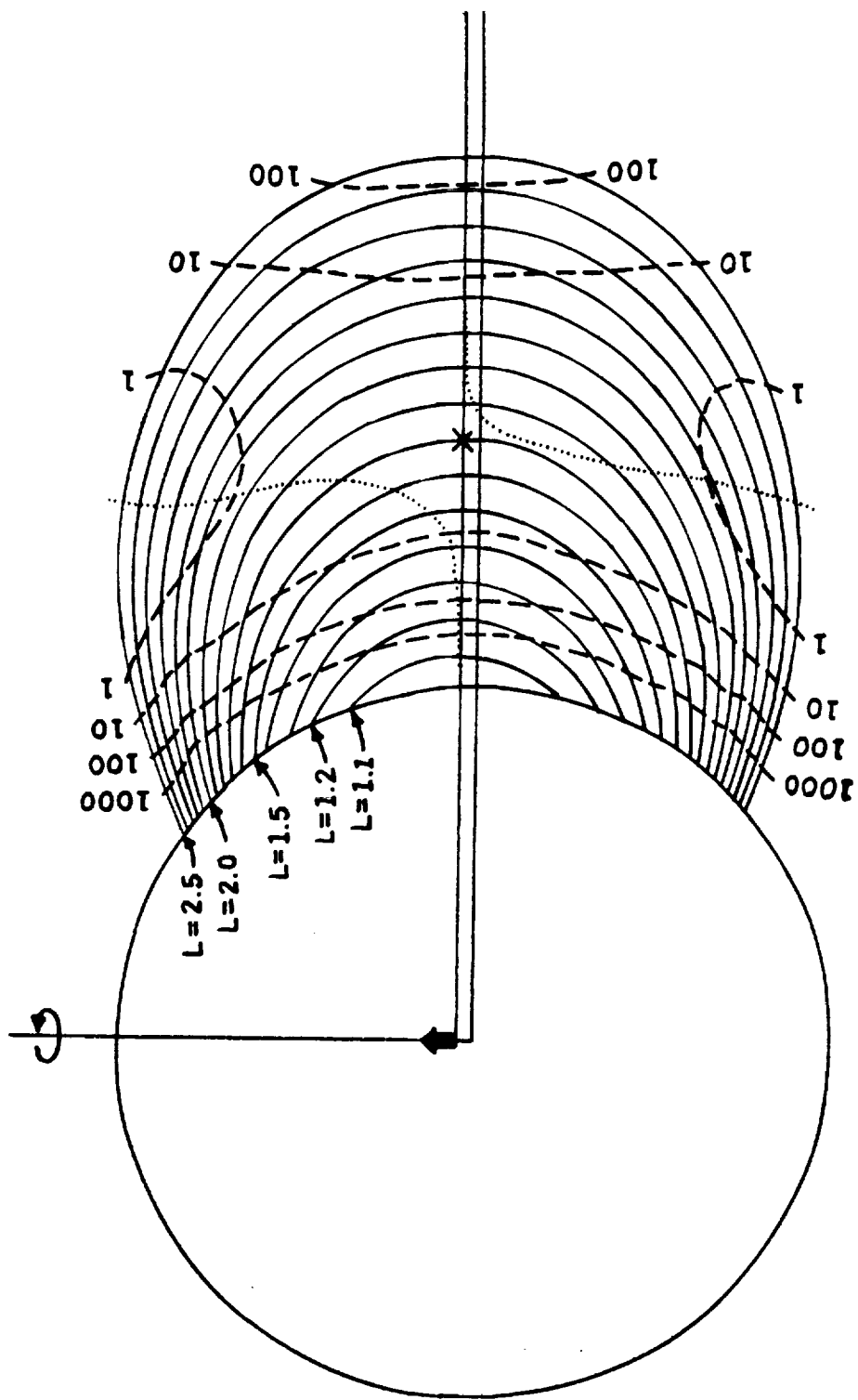


Fig.3. Contour Plot of electron density in the meridional planes of Northern and Southern Hemispheres for equinox conditions. The solid lines are dipole field lines whereas the broken lines are contours of constant electron density. The dotted lines are loci of points at which the components of gravitational and centrifugal forces along the field lines are equal and opposite. The cross mark represents the saddle point in the electron density profile.

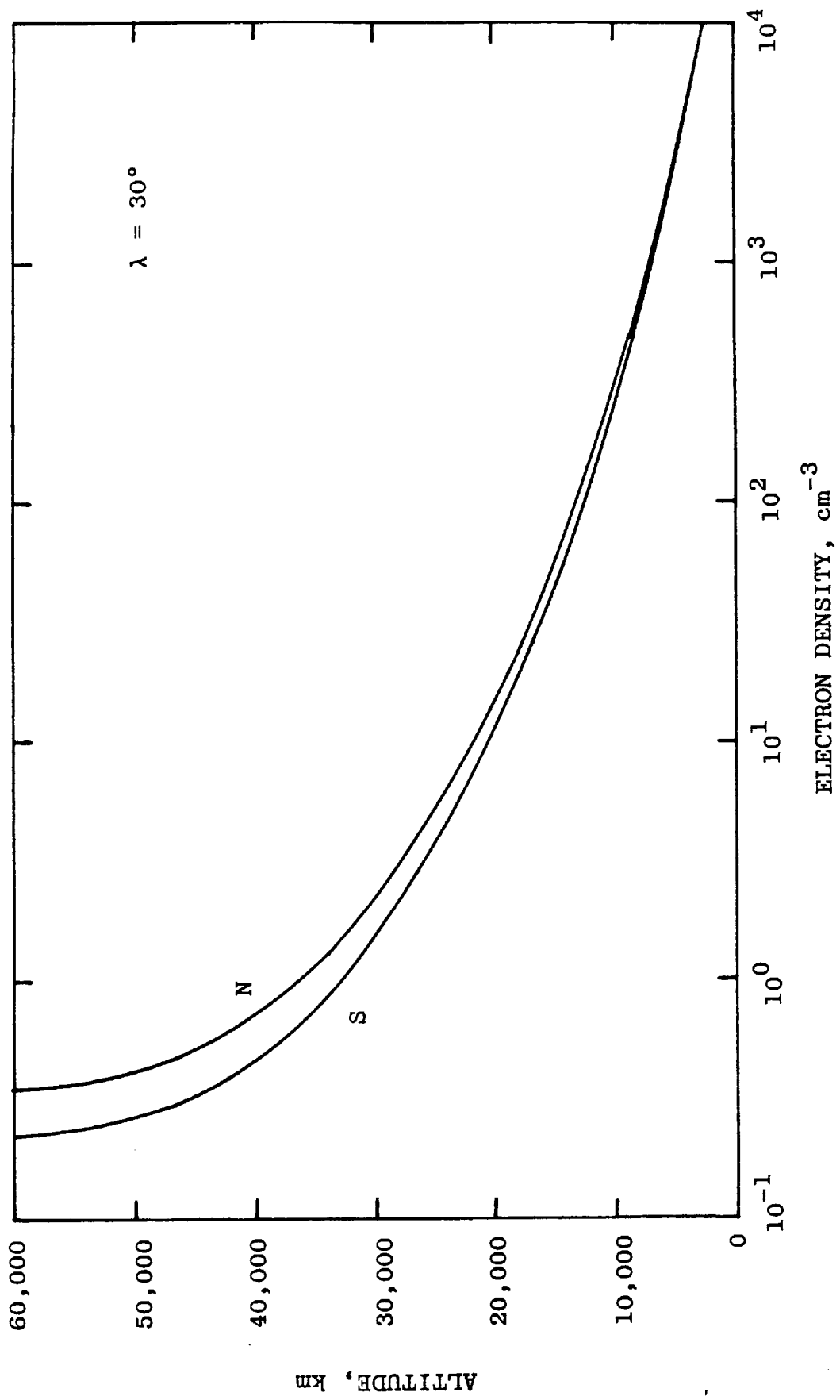


Fig.4. Vertical profiles of electron density at midlatitude locations ($\lambda = 30^\circ$) in the Northern and Southern hemispheres for equinox conditions.

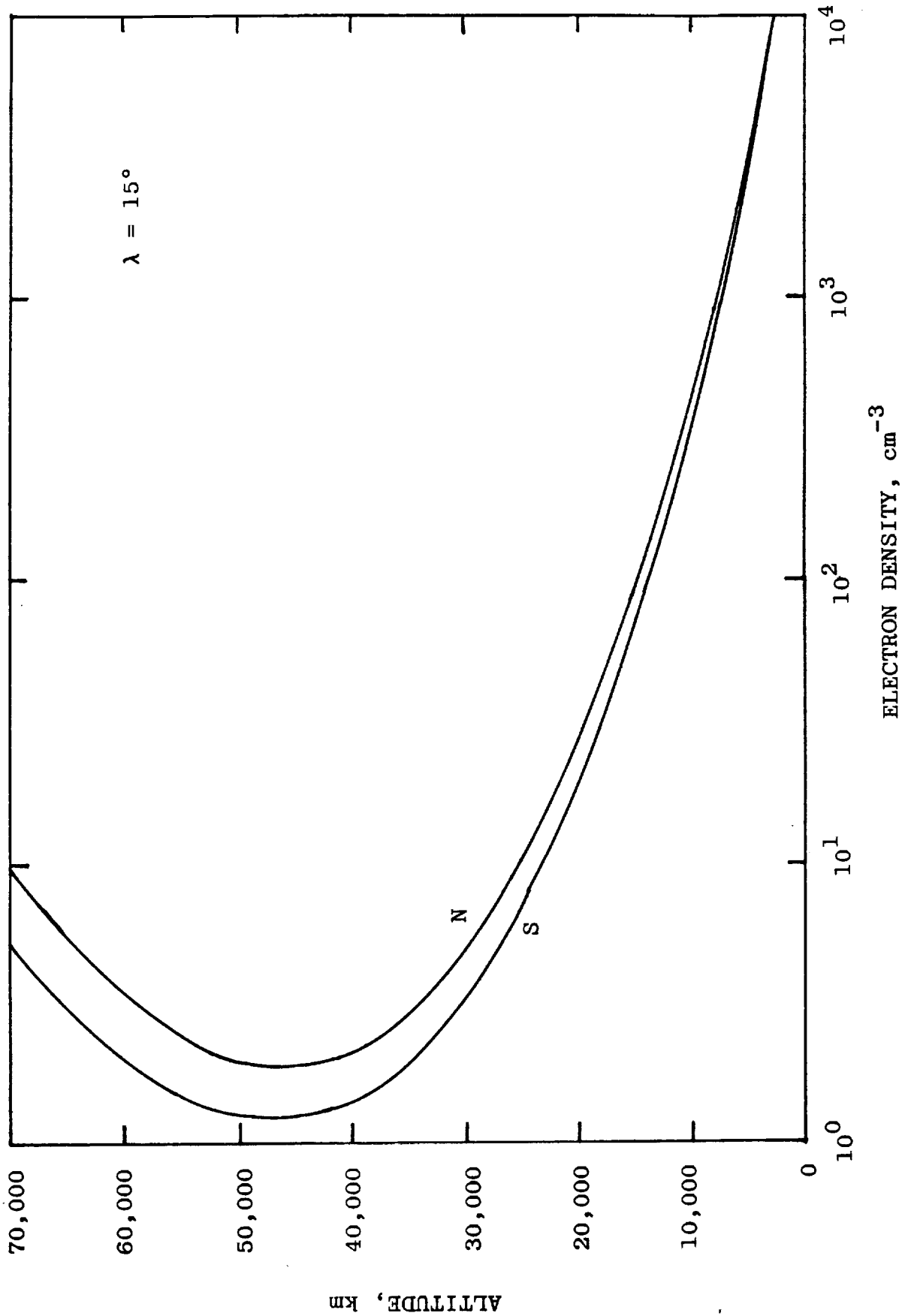


Fig. 5. Vertical profiles of electron density at low latitude locations ($\lambda = 15^\circ$) in the Northern and Southern hemispheres for equinox conditions.

Saturn's Plasmasphere in Offset Dipole Model*

A Tan (Department of Physics, Alabama A&M University,
Normal, AL 35762; 205-851-5313)

The magnetic field of Saturn can be approximated by that of a dipole coaxial with the rotational axis and displaced from the center northward by a distance of $0.05 R_S$, R_S being the reference radius of Saturn. A diffusive equilibrium model of Saturn's ionosphere for equinox conditions is constructed to study the offset effect of this dipole. Because of the field line alignments, the electron densities are generally greater in the northern hemisphere than in the southern. The plasma scale heights are also greater in the northern hemisphere. There is plasma pileup at higher heights above the equator, owing to the centrifugal dispersion of ionization there.

*This study was supported by NASA Grant NAGW-1067.

1.1991 Spring Meeting

2.000607177

3.(a) Box 447
Normal, AL 35762

(b) 205-851-5313

4.SA

5.(a)
(b) 5729 Ionospheres
(c)

6.PO

7.0%

8.\$50 check enclosed

9.C

10.Request PO (Publication only)
I shall not be able to attend

11.No